Strength of Topologically Induced Magnetic Moments in a Quantum Device

P. Exner, P. Šeba, and A. F. Sadreev*
Nuclear Physics Institute, Academy of Sciences of the Czech Republic, 250 68 Řež near Prague, Czech Republic
and Doppler Institute, Czech Technical University, Břehová 7, 115 19 Prague, Czech Republic

P. Středa and P. Feher
Institute of Physics, Academy of Sciences of the Czech Republic, Cukrovarnická 10, 162 00 Prague, Czech Republic
(Received 9 July 1997)

We consider resonant vortices around nodal points of the wave function describing electron transport through a mesoscopic device. With a suitable choice of the device geometry, the dominating role is played by single vortices with a preferred orientation. To characterize the strength of the resulting magnetic moment, we have introduced a "magnetance," the quantity defined in analogy with the device conductance. Its basic properties and possible experimental detection are discussed. [S0031-9007(97)05255-1]

PACS numbers: 73.20.Dx, 47.32.–y, 73.50.Yg

The topological structure of quantum mechanical wave functions is responsible for many observable phenomena. One of its prominent consequences is the existence of vortices. They have already been observed in macroscopic quantum systems, rotating superfluid helium, and superconductors. In general, their existence is connected with the time reversal symmetry breaking. The first example of such a topological effect was already given in the very early days of the quantum theory. It concerns the probability current density of a single electron defined conventionally by

$$\vec{j}(\vec{r}) = (\hbar/m^*)\,\mathrm{Im}\,[\bar{\psi}(\vec{r})\vec{\nabla}\psi(\vec{r})], \qquad (1)$$

which may be nontrivial once the wave function ψ is complex. In systems with open geometry a nonzero probability current refers to an electron transport through the system, i.e., from the source to a drain. Dirac [1] pointed out that the quantum probability current may exhibit a vortex structure around nodal points (zeros) of the corresponding wave function. The effect was later discussed by Hirschfelder [2]. Recently it has been demonstrated numerically that the current in topologically nontrivial devices exhibits pronounced vortices the form and magnitude of which changes quickly with the energy [3–7] and applied magnetic field [8]. The experimental evidence of their existence is of particular interest.

The direct consequence of a vortex is a nonzero magnetic moment, which has to depend on the applied current in a similar way as the device conductance. The natural physical quantity representing a vortex structure strength is thus the device "magnetance" given by the ratio of the magnetic moment and applied voltage drop. To analyze the effect of vortices to the electron transport and magnetance we will limit our consideration to devices with two-dimensional gas of spinless electrons. Main attention will be payed to the simple device formed by a piece of the one-dimensional wire with tangentially attached circular cavity (a quantum dot) as sketched in Fig. 1. It may be expected that there appears a dominating circulating current in analogy with the classical gas flow. This structure is thus the natural candidate for an experimental attempt to observe electron vortices.

The vortices are closely related with the topological structure of the phase. To be more explicit, let us write the wave function as

$$\psi = \sqrt{\rho}\, e^{iS}, \qquad (2)$$

where ρ is the probability density of the particle and S is the corresponding phase. The latter is defined modulo

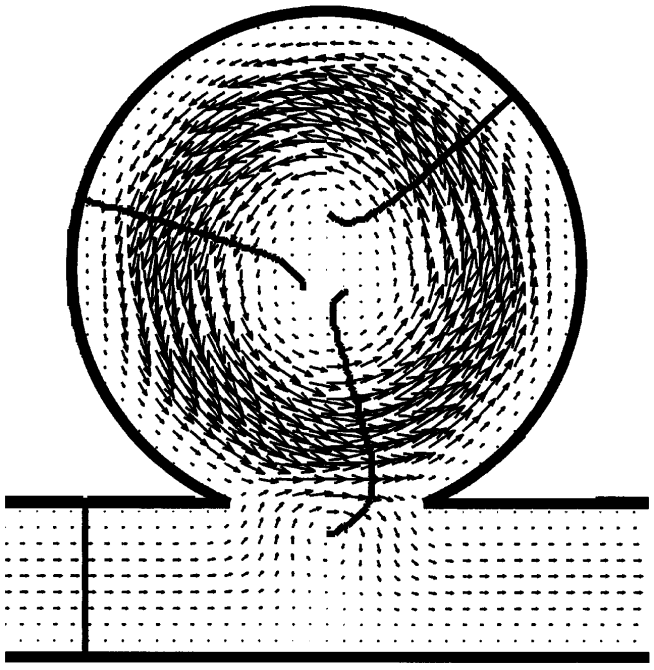

FIG. 1. The model device geometry with phase cuts (solid lines) for the energy indicated in Fig. 2 by the arrow. The window between the wire and the cavity equals 5/4 of the wire width w and the cavity radius $R = 5w/3$. Corresponding current density is illustrated by arrows.

 0031-9007/98/80(8)/1710(4)$15.00

2π and assumes conventionally values in the interval $[0, 2\pi)$. In the two-dimensional case it is possible to identify the configuration space with a region in the complex plane and to treat a possible multivaluedness of S in terms of its analytical structure, especially cuts and branching points corresponding to different Riemannian sheets of this function.

Existence of a branching point on the phase Riemannian surface implies appearance of a vortex in the corresponding quantum probability flow [2]. Inserting (2) into (1) we get

$$\vec{j}(\vec{r}) = \frac{\hbar}{m^*}\rho(\vec{r})\vec{\nabla}S(\vec{r}). \tag{3}$$

The vector $\vec{v} = (\hbar/m^*)\vec{\nabla}S$ can be regarded as a velocity of the corresponding probability flow. For a closed curve Γ the vorticity of $\vec{v}$ along Γ is thus

$$\oint_\Gamma \vec{v}\, d\vec{l} = \frac{\hbar}{m^*}\delta S = 2\pi\frac{\hbar}{m^*}m; \qquad m = 0, \pm 1, \pm 2, \ldots, \tag{4}$$

where δS is the phase change when winding once around the curve. Since the wave function (2) must be single valued, the difference δS can only be equal to a multiple of 2π. If the phase S has no singularities inside Γ, the contour can be shrunk into a point in which case the vorticity is zero. If, on the other hand, Γ encircles a nodal point of ψ, the phase is ambiguous at this point and the integer m may be nonzero. In this situation the corresponding probability current exhibits a vortex centered at the nodal point.

In quantum devices three basic topological situations can occur (see Fig. 1):

(a) A phase cut starts and ends at the boundary of the system. This is typical for integrable systems. As a simple example, consider the transport through a straight quantum waveguide of the width w parallel to the x axis. If the incident wave is in the nth transverse mode, the wave function has the form

$$\psi_{k,n}(x, y) = \sqrt{\frac{1}{\pi w}}\, e^{ikx} \sin\frac{\pi n y}{w}, \tag{5}$$

where n is the mode number and $\hbar^2(k^2 + \pi^2 n^2/w^2)/2m^*$ is the particle energy. In this case the phase $S = kx$ is monotonically increasing in the longitudinal direction and its cuts are located at the segments $x = 2\pi j/k$, $j = \ldots, -1, 0, 1, \ldots$, parallel to the x axis. Their end points lie at the boundary $y = 0, w$. They are physically irrelevant being not branching points.

(b) The cut starts at the boundary and ends at some nodal point inside the system. The internal end point is a branching point which is related to a single vortex.

(c) The cut connects two nodal points of the wave function. Both end points are branching points which correspond to a pair of vortices rotating in opposite directions.

To define the vortex magnetance we will follow the scattering approach [9], generally accepted in the transport theory of quantum devices. To establish conductance of a two-terminal device, infinitely long ideal leads are placed between the device (scattering region) and electron reservoirs (source and drain) allowing an explicit asymptotic form of scattering wave functions. The obtained transmission coefficient $T(E)$ is used to relate the applied current J and the chemical potential difference between reservoirs $\Delta\mu$. In the limiting case of vanishing $\Delta\mu$ and at zero temperature the electron transport is determined by properties of electrons at the Fermi energy E_F, and we have

$$J = \frac{e}{h}T(E_F)\Delta\mu. \tag{6}$$

The applied current is responsible for a nonzero angular momentum of the system. It can be divided into two parts: momentum of the center of mass and the momentum due to electron motion relative to the center of mass. The later one originates in circulating currents giving rise to a magnetic moment $\vec{M} \equiv (0, 0, M)$ representing their strength. Angular momentum of the center of mass is controlled by the current density within the ideal leads only.

In the simplest case of one-dimensional ideal leads having a common axis the angular momentum of the center of mass can easily be evaluated. It is controlled by the product $T(E_F)g_0(E_F)\vec{j}_0(\vec{r})$ with $g_0(E_F)$ and $\vec{j}_0(\vec{r})$ being the density of states and current density, respectively, within the system without the scattering region (the device is replaced by the lead). In this case we get the vortex magnetance in the following form:

$$\frac{\vec{M}(E_F)}{\Delta\mu} = \frac{e}{2c}\int \left(g(E_F)\vec{j}(\vec{r}) - T(E_F)g_0(E_F)\vec{j}_0(\vec{r})\right) \times \vec{r}\, d^2r, \tag{7}$$

where $g(E)$ denotes the density of states of the considered system. The magnetance defined in this way characterizes the vortex structure of the studied device and it is invariant with respect to coordinate system translations.

The expression, Eq. (7), is applicable to the device sketched in Fig. 1. To stress the effect of the device geometry the flat potential is assumed within the device area demarcated by hard walls. The relevant wave functions are thus eigenfunctions of the free-electron Schrödinger equation with zero values at the boundaries.

To estimate the magnetance of the considered device, let us first summarize wave function properties of the separated circular cavity. In polar coordinates eigenfunctions are determined by zeros of Bessel functions J_m at the cavity radius R and we have

$$\psi^{\pm}_{l,m}(r, \theta) = c_{l,m}J_m(k_{l,m}r)e^{\pm im\theta}, \tag{8}$$

where $k_{l,m} = x_{l,m}/R$ with $x_{l,m}$ being the lth zero of the Bessel function J_m, and $c_{l,m}$ is the normalization factor. The quantum number m ($m = 0, 1, 2, \ldots$) represents the angular momentum $\pm(\hbar/m^*)m$ which is closely related to the vorticity defined by Eq. (4). The eigenstates of

spinless electrons are twofold degenerated with respect of the sign of the momentum.

Only the azimuthal component of the probability current density for given eigenenergy $E_{l,m}$ might be nonzero, and it is given as follows:

$$j_\theta(r) = A_{l,m} \frac{\hbar}{m^*} \frac{m}{r} c_{l,m}^2 J_m^2(k_{l,m} r), \qquad (9)$$

where $A_{l,m}$ is given by the difference of weight factors, $A_{l,m} = |a_{l,m}^{(+)}|^2 - |a_{l,m}^{(-)}|^2$, representing amplitudes $a_{l,m}^{(+)}$ and $a_{l,m}^{(-)}$ of eigenfunctions with positive and negative values of the orbital momentum, respectively. In the equilibrium case the problem has time reversal symmetry requiring equality of weight factors and the total momentum vanishes.

Attaching a wire the wave functions $\psi(r,\theta)$ given by Eq. (8) become modified by a coupling with plane waves. Assuming a small window between wire and cavity, much less than R, wave functions $\psi(r,\theta)$ will be only slightly modified. The main effect will be a level broadening represented by the spectral density $g_{l,m}(E)$ with sharp maxima at energies $E \cong E_{l,m}$. Wave functions representing states with the same direction of the probability flow in the window region will be much more easily matched together than those with opposite flow directions. In the current currying regime the amplitude of cavity wave functions matched with incident plane wave will be thus enhanced giving rise to circulating currents. Corresponding magnetance may be estimated by choosing a proper value of the $A_{l,m}(E)$ entering Eq. (9). Inserting the current density $j_\theta(r)$, Eq. (9), into the expression for the magnetance, Eq. (7), we get

$$\frac{M(E_F)}{\Delta\mu} \cong \mu_B^* \sum_{l,m} A_{l,m}(E_F)\, m\, g_{l,m}(E_F), \qquad (10)$$

where $\mu_B^* = e\hbar/2m^*c$ is the effective Bohr magneton. Because of the dominating role of the spectral density $g_{l,m}(E)$ a resonance character of the magnetance is expected. Since $g_{l,m}(E)$ is proportional to m^* the magnetance is of the purely topological origin.

As an example, the energy dependence of the magnetance and the transmission coefficient close to the resonance for $l = 1$ and $m = 3$ is shown in Fig. 2. The corresponding current density distribution for E_F indicated by arrows is presented in Fig. 1. Four phase-cut end points represent vortex centers. Three of them are located close to the cavity center giving rise to pronounced circulating current. For a fixed window region the broadening of cavity levels becomes weaker for larger radius R giving rise to more pronounced resonances as seen in Fig. 3(a). For $R > 1.8\,w$ a more complicated resonance structure appears due to states with different quantum numbers l.

For a quite well separated resonance the magnetance peak height may be estimated by equality of the current originated in the cavity eigenfunction, Eq. (8), and that of the single wire, Eq. (5), in the common region, i.e., in

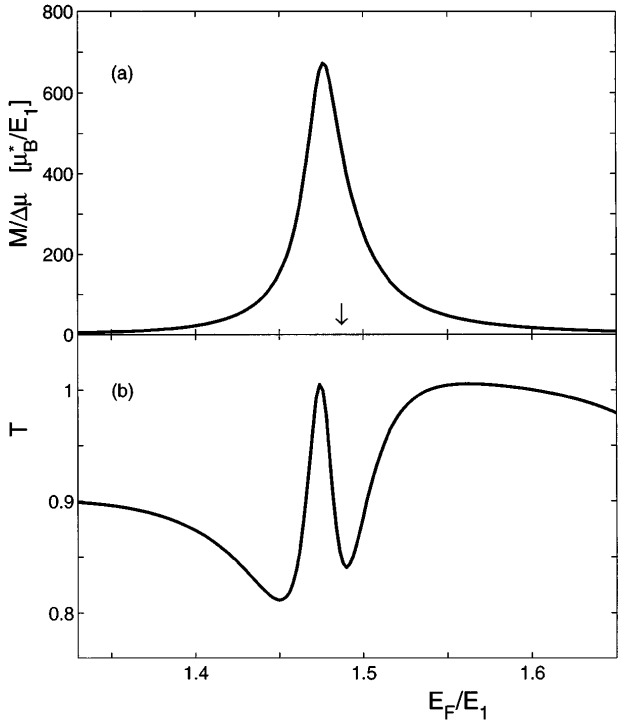

FIG. 2. Energy dependence of the magnetance $M/\Delta\mu$ (a) and transmission coefficient T (b) in the vicinity of the resonance for $l = 1$ and $m = 3$. Device geometry is the same as that in Fig. 1 and E_1 denotes the energy of the lowest transversal mode $E_1 = \pi^2\hbar^2/2m^*w^2$.

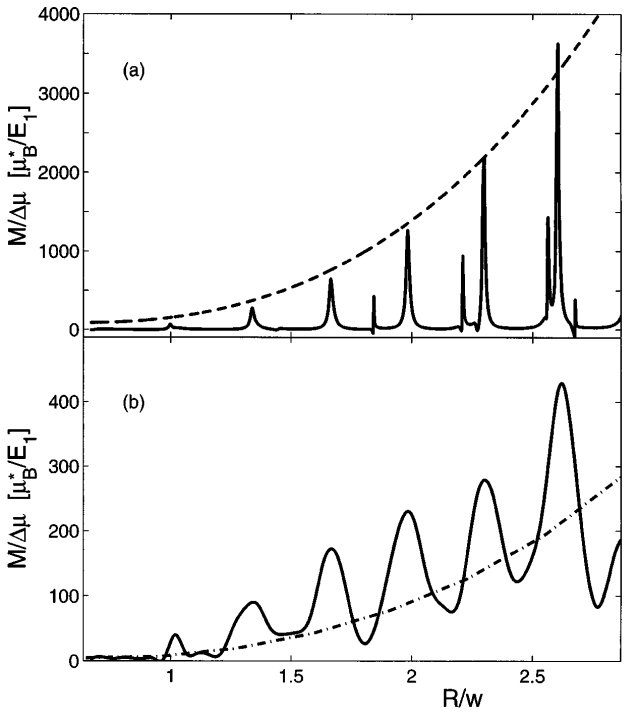

FIG. 3. Magnetance $M/\Delta\mu$ at zero temperature (a) and at the temperature $0.05\,E_1/k_B$ (b) as function of the cavity radius for fixed window width $5w/4$. The dashed line represents estimation for resonance maxima, Eq. (11). The dash-dotted line is the result of the semiclassical treatment.

the area of overlapping circular and strip regions. This condition gives

$$A_{l,m}(E_r)\,\frac{\hbar g(E_r)}{m^*}\,m\int_{R-d}^{R} c_{l,m}^2 J_m^2(k_{l,m}r)\,\frac{dr}{r} \cong \frac{1}{h}\,\frac{1}{\pi w}\int_{w-d}^{w}\sin^2\frac{\pi y}{w}\,dy\,, \quad (11)$$

where d is the width of the common region, $d = w + R - y_0$, with y_0 being the distance of the cavity center from the bottom wire edge. This estimation is in good agreement with the values obtained by direct evaluation of Eq. (7), as shown in Fig. 3(a).

The above amplitude estimation, Eq. (11), assumes an *ideal* coupling allowing an easy transfer of the incident wave with transmission coefficient T approaching unity. Out of the ideal coupling a reflection will take place and T will decrease. However, far enough from the resonance the mixing of plane waves with eigenfunction of the separated cavity becomes less effective and transmission will be enhanced. This typical energy dependence is shown in Fig. 2(b).

At finite temperatures the magnetance is given by the following expression:

$$\frac{M(\mu,T)}{\Delta\mu} = -\frac{1}{\Delta\mu}\int\frac{\partial f_0(E)}{\partial\mu}\,M(E)\,dE\,, \quad (12)$$

where $f_0(E)$ denotes the Fermi-Dirac distribution function and $M(E)$ is the zero temperature magnetic moment given by Eq. (7). The resulting magnetance at a nonzero temperature is shown in Fig. 3(b). For high enough temperatures resonances will fully be smeared out and the magnetance should approach values obtained by a semiclassical treatment. Since the averaged density of states g scales with the cavity area $\langle g\rangle \cong (m^*/h\hbar)E_F\,\pi R^2$ and $m \sim R/w$, the approximate scaling of the magnetance with R^3 is expected.

The semiclassical description of the studied ballistic transport can be based on the billiard model [10]. Electrons are injected uniformly over the wire width w and with the probability $\frac{1}{2}\cos\phi$ along the direction represented by the angle ϕ with respect of the wire axis. As expected, the resulting magnetance, shown in Fig. 3(b), approaches mean values obtained by full quantum-mechanical treatment.

The same qualitative features of the magnetance are expected for any cavity defined by a potential of the circular symmetry. We have found that resonances are very stable with respect of the radius modulation ($\Delta R(\theta)/\langle R\rangle < 0.1$) and potential fluctuations less than the energy level separation of the unperturbed cavity. The electron-electron interaction, which was not taken into account, should not change the magnetance structure qualitatively.

Impurity potentials within the wire area have a destructive effect on the magnetance. They suppress the transmission coefficient and, consequently, the current flow along the window between wire and cavity, which is responsible for the magnetance peak height as discussed above, Eq. (11). They also give rise to additional vortices of the uncontrollable orientation within the wire region. The resulting richer magnetance structure can be very easily smeared out by the temperature. This destructive effect will be even more effective for wider, multimode, wires.

In real systems the probability to have impurities within the wire region might be lowered by shortening the wire length. A similar device, but with centrally attached wires represented by point contacts, has already been realized [11]. The proper design could also allow one to control cavity area by top gates. To observe resonances the energy level separation of the isolated cavity has to be larger than the thermal energy k_BT. For the device fabricated from a GaAs-AlGaAs heterostructure it limits the cavity radius, $R[\mu\mathrm{m}] < 0.2/\sqrt{T[K]}$. For example, assuming $R \sim 0.5\ \mu$m resonances could be indicated by a fluxmeter allowing measurements with accuracy $10^2\mu_B$, which is in principle within experimental reach [12]. The contribution of noncirculating currents cannot be easily excluded by experimental setup, as has been done in our theoretical treatment. Under the standard conditions of the fixed applied current it will be, however, responsible for a monotonic background only.

The research has been partially supported by the DTP Foundation as well as by Grants No. INTAS-RFBR 95–657 and No. AVČR A1048804. The support obtained from the Theoretical Physics Foundation in Slemeno is also greatly acknowledged.

*Permanent address: Institute of Physics, Academy of Sciences, 660036 Krasnoyarsk, Russia.

[1] P. A. M. Dirac, Proc. R. Soc. London A **133**, 60 (1931).
[2] J. O. Hirschfelder, J. Chem. Phys. **67**, 5477 (1977).
[3] K.-F. Berggren and Zheng-Li Ji, Phys. Rev. B **47**, 6390 (1993).
[4] S. Chaudhuri, S. Badyopadhyay, and M. Cahay, Phys. Rev. B **45**, 11 126 (1992).
[5] P. Exner, P. Šeba, M. Tater, and D. Vanek, J. Math. Phys. (N.Y.) **37**, 4867 (1996).
[6] V. M. Ramaglia, F. Ventriglia, and G. P. Zucchelli, Phys. Rev. B **48**, 2445 (1993); **52**, 8372 (1995).
[7] Hua Wu and D. W. L. Sprung, Phys. Lett. A **183**, 413 (1993).
[8] K. N. Pichugin and A. F. Sadreev, Zh. Eksp. Teor. Fiz. **109**, 546 (1996) [Sov. Phys. JETP **82**, 290 (1996)].
[9] D. S. Fisher and P. A. Lee, Phys. Rev. B **23**, 6851 (1981).
[10] C. W. Beenakker and H. van Houten, Phys. Rev. Lett. **63**, 1857 (1989).
[11] B. J. van Wees, L. P. Kouwenhoven, C. J. P. M. Harmans, G. J. Williamson, C. E. Timmering, M. E. I. Broekaart, C. T. Foxon, and J. J. Harris, Phys. Rev. Lett. **62**, 2523 (1989).
[12] A. K. Geim, S. V. Dubonos, I. V. Grigorieva, J. G. S. Lok, J. C. Maan, X. Q. Li, F. M. Peeters, and Yu. V. Nazarov, in "Superlattices and Microstructures" (to be published).